Generating dual beams from a single steerable parametric loudspeaker

Chuang Shi[a,*], Yoshinobu Kajikawa[a], Woon-Seng Gan[b]

[a] *Department of Electrical and Electronic Engineering, Kansai University, Osaka, Japan*
[b] *School of Electrical and Electronic Engineering, Nanyang Technological University, Singapore*

Abstract

The parametric loudspeaker utilizes an ultrasonic transducer array to transmit a directional sound beam in air based on the parametric array effect. In recent studies, phased array techniques have been applied to achieve controllable directivity patterns or to change the direction of the sound beam. Such a parametric loudspeaker is often referred to as a steerable parametric loudspeaker. In this paper, a dual beam generation method is elaborated. It aims to transmit two sound beams from just one steerable parametric loudspeaker. The two sound beams carries the same audio content to different locations. This dual beam generation method is compatible with the configuration of existing steerable parametric loudspeakers based on phased array techniques. As an algorithm solution, the dual beam generation method readily improves the flexibility of the steerable parametric loudspeaker.

Keywords: Parametric loudspeaker, Ultrasonic transducer array, Beamsteering, Spatial aliasing

*Corresponding Author's Email: r148005@kansai-u.ac.jp

1. Introduction

Yoneyama *et al.* was credited to the invention of the parametric loudspeaker in 1983 [1], but the sound principle of the parametric loudspeaker, namely the parametric array effect, was discovered in the early 1960s [2, 3]. When two primary frequencies (PFs) are transmitted from an ultrasonic transducer, new frequency components, such as the difference frequency (DF), sum frequency, and higher order harmonics, are generated due to nonlinear acoustic effects. Furthermore, as a result of the absorption in air, the PFs, sum frequency, and higher order harmonics decay more rapidly than the DF [4]. More importantly, the DF is audible and still exhibits a narrow directivity pattern, which can be modeled by an end-fire array of virtual sources [2, 5].

With the ability to generate directional sounds, the parametric loudspeaker has been attempted in various applications for creating personalized listening experience. For instance, the parametric loudspeaker has been deployed in mobile devices to replace present wearable solutions, such as headphones and earphones, preventing the reproduced sound from diffusing into the surrounding area [6]. In active noise control, using the parametric loudspeaker as the control source has also demonstrated the feasibility to suppress the noise level in a moving zone without causing spillover [7]. There is no doubt that the parametric loudspeaker has become a competitive add-on to the traditional entertainment and media. An audio visualization system, as well as a non-contactable musical instrument, has been implemented using parametric loudspeakers [8, 9]. The PFs are cleverly involved to trigger light emitting diodes and create the acoustic radiation force to allow users to be

able to interact with sounds using their eyes and hands.

However, there are two acknowledged drawbacks of the parametric loudspeaker, *i.e.* the notable harmonic distortion [10] and relatively weak bass output [11]. Research works on preprocessing methods have been extensively carried out to address the harmonic distortion [12, 13, 14, 15]. On the other hand, the bass output of the parametric loudspeaker is an inevitable result of the parametric acoustic array. Hence, a combination of the conventional and parametric loudspeakers has been more frequently mentioned [16]. This combination allows the conventional loudspeaker to play a complementary role in the bass output. It also provides a solution to the dilemma that dispersive and directional sound fields cannot be accurately reproduced from a stereo loudspeaker system at the same time.

Recently, several directivity control methods have been investigated for the parametric loudspeaker, in order to meet an increasing range of applications. Olszewski *et al.* [17] have implemented a hybrid system to change the direction of the sound beam. They have found that the motorized frame has better beamsteering ability than phased array techniques when the inter-channel spacing is a few centimeters. However, the hybrid system has to solve reflections between neighboring channels and the motorized frame makes the overall size bulky. Gan *et al.* [18] have worked out a compact configuration of the steerable parametric loudspeaker. When the ultrasonic transducers have a diameter of 1 cm, the inter-channel spacing is reduced to about 0.58 times the wavelength of a 40 kHz carrier. This compact configuration is efficient to avoid spatial aliasing of the PFs, although it has been discovered in simulations and experiments that spatial aliasing of the PFs does not neces-

sarily cause spatial aliasing of the DF [19]. This phenomenon is called the grating lobe elimination, whereby the inter-channel spacing of the steerable parametric loudspeaker is allowed to be even larger than the wavelength of the ultrasonic carrier.

The motivation of this paper is to challenge the limitation that one steerable parametric loudspeaker is able to transmit just one controllable sound beam. It has been unsuspected that multiple parametric loudspeakers are necessary for the generation of multiple sound beams [20]. Takeoka and Yamasaki [21] have programmed 192 individual delay units in a field programmable gate array (FPGA) to drive a corresponding number of ultrasonic transducers, where different sound beams are supposed to be generated from different groups of the ultrasonic transducers. Such a method is essentially the same as using multiple steerable parametric loudspeakers. It leads to high power consumption, since more ultrasonic transducers and amplifiers are powered up [22]. Moreover, spatial aliasing incurred in the generation of multiple sound beams presents a complicated problem to be formulated.

For simplicity, we explains in Section 2 the spatial aliasing problem when two steerable parametric loudspeakers are used together and elaborate a dual beam generation method that requires just one steerable parametric loudspeaker. Subsequently, boundary conditions are discussed for the dual beam generation method in Section 3. In Section 4, the experiment results using different configurations of the steerable parametric loudspeaker are presented. Lastly, the contributions of this paper is concluded in Section 5.

2. Dual Beam Generation

As aforementioned, phased array techniques have been validated to be effective in the steerable parametric loudspeaker. The theoretical basis of previous works is provided by the product directivity principle [23, 24]. It implies that the directivity pattern of the DF can be roughly computed by the product of the directivity patterns of the PFs. Therefore, when the PFs are transmitted in one direction, the DF wave resultant from the parametric array effect is found to appear in the same direction. There is a recent development of the directivity model that adds a convolution operation with the Westervelt's directivity, which has been demonstrated to have a higher accuracy [5]. Therefore, this paper utilizes the new convolution model in all the simulations.

The application background of the dual beam generation is explained here. A directional sound system that allows users to switch between one and two sound beams is illustrated in the scenario of Fig. 1. A hearing-impaired listener is watching a television program together with other listeners with normal hearing. This scenario is common in Asian countries where three generations live together. In order to enhance the listening experience of the hearing-impaired listener, a parametric loudspeaker delivers the enhanced audio content to him without increasing sound input to the rest of listeners. When another hearing-impaired listener joins in, an additional sound beam would be needed. In this situation, the directional sound system with the flexibility to generate one or two sound beams becomes a favorable solution.

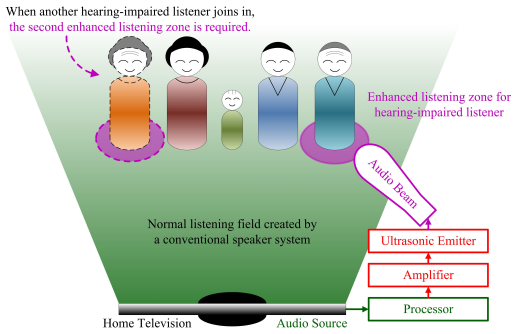

Figure 1: Application scenario of a directional sound system that is flexible to generate one or two steerable sound beams.

2.1. Using two steerable parametric loudspeakers

Two steerable parametric loudspeakers are used to transmit two sound beams in directions that are denoted by θ_a and θ_b. As shown in Fig. 2, each steerable parametric loudspeaker is in charge of transmitting one sound beam. Assume that each steerable parametric loudspeaker consists of M channels. The delay amount of each channel is computed by the delay and sum beamforming, *i.e.* $\tau_m^a = md\sin\theta_a/c_0$ and $\tau_m^b = md\sin\theta_b/c_0$ for $m = 0, 1, \ldots, M-1$, where d is the inter-channel spacing and c_0 is the speed of sound. The directivity pattern of the PF is therefore computed by the superposition of two directivity patterns as

$$H(k,\theta) = \sum_{m=0}^{M-1} w_m \left[e^{jmdk(\sin\theta - \sin\theta_a)} + e^{jmdk(\sin\theta - \sin\theta_b)}\right] \tag{1}$$

where k is the wavenumber of the PF.

There are two disadvantages of using two steerable parametric loudspeakers together. Firstly, the sound pressure level of the DF wave is reduced as the effective size of the steerable parametric loudspeaker is halved from that

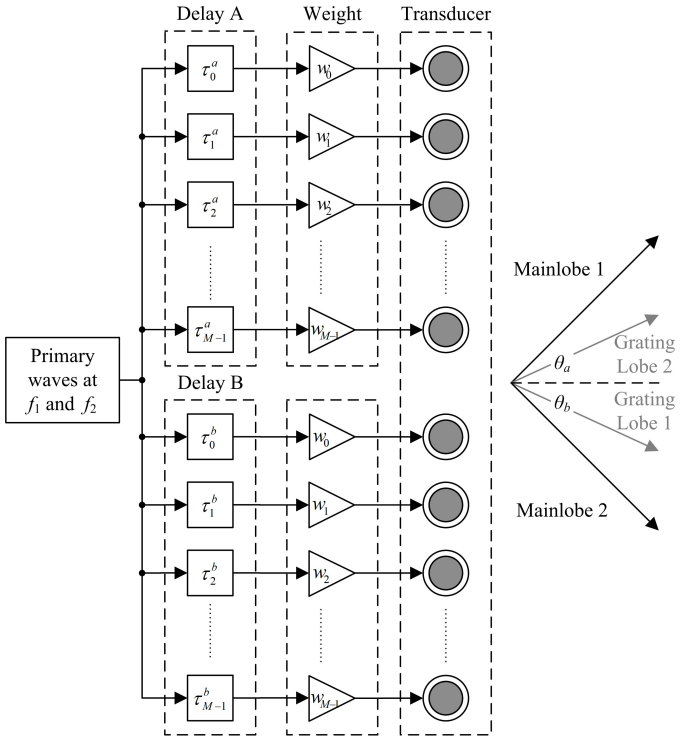

Figure 2: Block diagram of using two steerable parametric loudspeakers for dual-beam generation, where each steerable parametric loudspeaker provides one sound beam.

of using two steerable parametric loudspeakers as a whole. This also affects the beamwidth of each sound beam, since the aperture size is halved as well. Secondly, using two steerable parametric loudspeakers leads to a complicated spatial aliasing problem. To illustrate the spatial aliasing problem, simulations are carried out. Equal weights are adopted and the total power is fixed. Each steerable parametric loudspeaker consists of $M = 8$ channels. When two steerable parametric loudspeakers are used together, they provide $M_{combine} = 16$ channels. The upper PF varies increasingly from 40.25 kHz to 45 kHz and the lower PF varies decreasingly from 39.75 kHz to 35 kHz.

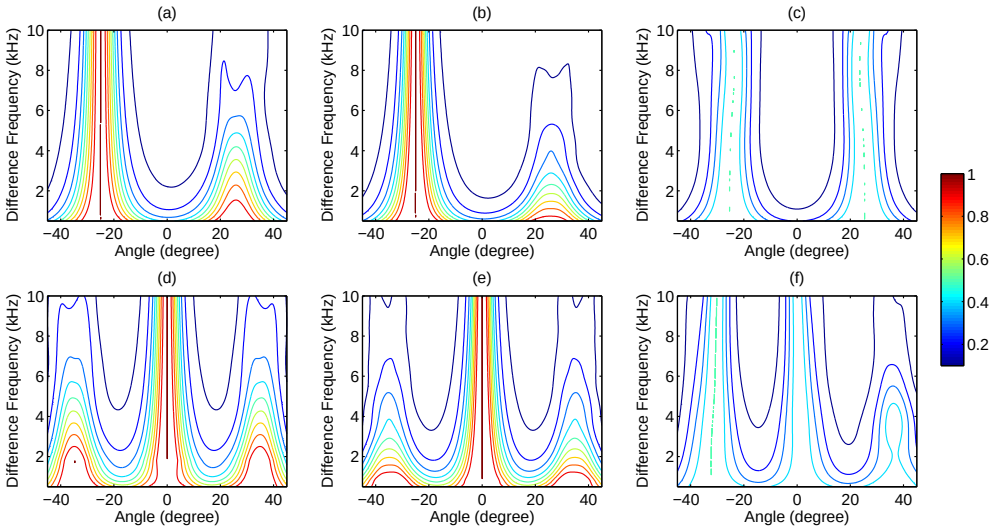

Figure 3: Using two steerable parametric loudspeakers to generate sound beams: (a) $d = 1$ cm, $M = 8$, $\theta_a = -25°$; (b) $d = 1$ cm, $M_{combine} = 16$, $\theta_a = -25°$; (c) $d = 1$ cm, $M = 8$, $\theta_a = -25°$ and $\theta_b = 25°$; (d) $d = 1.5$ cm, $M = 8$, $\theta_b = 0°$; (e) $d = 1.5$ cm, $M_{combine} = 16$, $\theta_b = 0°$; (f) $d = 1.5$ cm, $M = 8$, $\theta_a = -30°$ and $\theta_b = 0°$. When θ_a or θ_b is not specified, there is only one sound beam transmitted.

Hence, the DF is generated between the upper and lower PFs and ranges from 0.5 kHz to 10 kHz. The observable range of angles is set from $-45°$ to $45°$. Within in this range, the ultrasonic transducers are assumed to be omni-directional.

Firstly, the inter-channel spacing is set to $d = 1$ cm. Fig. 3(a) shows the directivity patterns of the DF when one steerable parametric loudspeaker transmits one sound beam at $-25°$. Fig. 3(b) shows two steerable parametric loudspeakers transmitting one sound beam together at $-25°$. The beamwidth becomes narrower. Fig. 3(c) shows how each steerable paramet-

ric loudspeaker is in charge of transmitting one sound beam. The grating lobe of one steerable parametric loudspeaker interferes with the mainlobe of the other steerable parametric loudspeaker. In particular, the steering angles of the DF wave at 8 kHz have been distorted from $\pm 25^\circ$ by 6%. Similarly, Figs. 3(d)-(e) show the directivity patterns of the DF when just one sound beam is transmitted at 0°, and Fig. 3(f) shows the other sound beam transmitted at -30°. Spatial aliasing is severe in Fig. 3(f) due to the large inter-channel spacing. These simulation results confirm that using two steerable parametric loudspeakers together can result in a complicated spatial aliasing problem as well as inaccurate steering angles.

2.2. Using one steerable parametric loudspeakers

To address the aforementioned disadvantages, the dual beam generation method has been proposed using just one steerable parametric loudspeaker as shown in Fig. 4 [16, 25]. The steerable parametric loudspeaker consists of M channels, but different delay amounts (τ_{m1} and τ_{m2} for $m = 0, 1, 2, \ldots, M-1$) are implemented for the PFs at f_1 and f_2. Therefore, the mainlobes of the two PFs are transmitted at θ_1 and θ_2, respectively. Note that θ_1 and θ_2 are different from the intended directions θ_a and θ_b. In the dual beam generation method, one of the two sound beams is resultant from the mainlobes of the PFs, while the other sound beam is generated by making use of the grating lobes of the PFs.

The dual beam generation method is briefly derived as follows. The mainlobe and the first grating lobe of the PFs are presumed to be symmetric to θ_s. Considering the fact that the spatial aliasing period gives the separation in normalized angles between the mainlobe and the first grating lobe, the

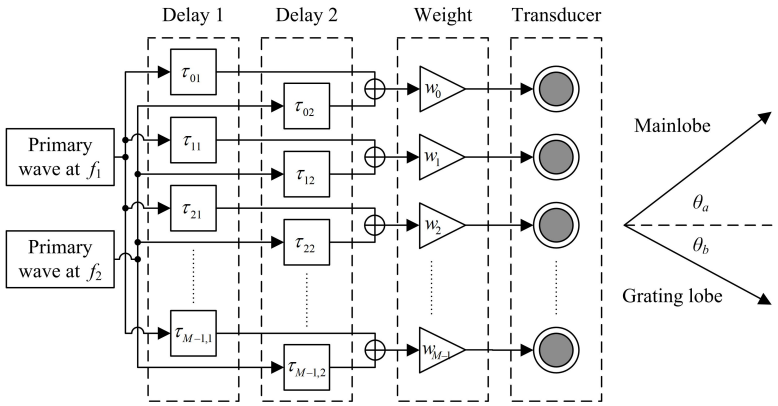

Figure 4: Illustration of a potential application of the steerable parametric loudspeaker which is able to generate both a single beam and dual beams.

mainlobes of the PFs are certainly found at

$$\sin\theta_1 = \sin\theta_s - \frac{c_0}{2f_1 d} \tag{2}$$

and

$$\sin\theta_2 = \sin\theta_s - \frac{c_0}{2f_2 d}. \tag{3}$$

These two mainlobes of the PFs result in one of the two sound beams at

$$\sin\theta_a = \frac{\sin\theta_1 + \sin\theta_2}{2} = \sin\theta_s - \frac{c_0}{4f_1 d} - \frac{c_0}{4f_2 d}. \tag{4}$$

Similarly, the first grating lobes of the PFs result in the other sound beam at

$$\sin\theta_b = \sin\theta_s + \frac{c_0}{4f_1 d} + \frac{c_0}{4f_2 d}. \tag{5}$$

To subtract (4) from (5) yields a quadratic equation, *i.e.*

$$(\sin\theta_b - \sin\theta_a)\, f_c^2 - \frac{c_0}{d} f_c - (\sin\theta_b - \sin\theta_a)\, \frac{f_d^2}{4} = 0, \tag{6}$$

where $f_c = (f_1 + f_2)/2$ is called the center frequency of PFs; $f_d = f_2 - f_1$ is the DF; $\theta_a < \theta_b$ and $f_1 < f_2$ are both assumed without loss of generality.

The solution to (6) is written as

$$f_c = \frac{c_0 + \sqrt{c_0^2 + d^2 \left(\sin\theta_b - \sin\theta_a\right)^2 f_d^2}}{2d\left(\sin\theta_b - \sin\theta_a\right)}. \tag{7}$$

When $c_0 >> d\left(\sin\theta_b - \sin\theta_a\right) f_d$, (8) is approximated by

$$f_c \approx \frac{c_0}{d\left(\sin\theta_b - \sin\theta_a\right)}. \tag{8}$$

Eq. (8) is the control formula of the dual beam generation method. It presents an ease-of-use relation between the the center frequency, inter-channel spacing, and separation between the sound beams in normalized angles.

Simulations are carried out using the dual beam generation method. The steerable parametric loudspeaker consists of 8 channels and adopts equal weights. With a given inter-channel spacing and two directions of the sound beams, the center frequency is computed by (8). The DF is generated from 0.5 kHz to 10 kHz. Firstly, the inter-channel spacing is set to $d = 1$ cm. Figs. 3(a)-(c) show the directivity patterns of the DF when the two sound beams are transmitted at $\pm 25^\circ$, -40° and 10°, -50° and 0°, respectively. The separation between the sound beams are purposely kept to be 50°. As the symmetric axis θ_s moves from 0° to -25°, the center frequency has to be increased from 40.7 kHz to 44.9 kHz. Because the observable range of angles is set from -45° to 45°, the sound beam transmitted at -50° disappears in Fig. 3(c). The inter-channel spacing is subsequently increased to $d = 1.5$ cm. Figs. 3(d)-(f) show the directivity patterns of the DF when the

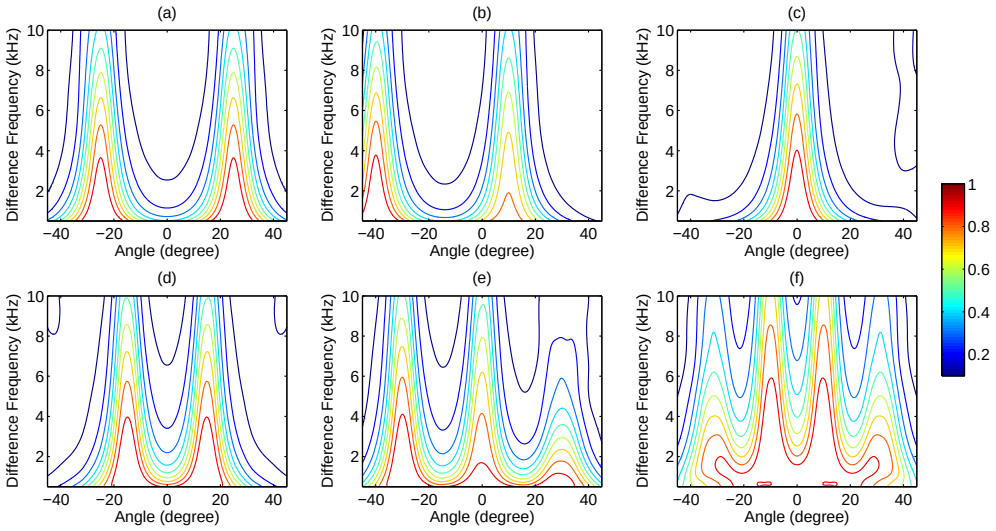

Figure 5: Using the dual beam generation method: (a) $d = 1$ cm, $f_c = 40.6$ kHz, $\theta_a = -25°$ and $\theta_b = 25°$; (b) $d = 1$ cm, $f_c = 42.1$ kHz, $\theta_a = -40°$ and $\theta_b = 10°$; (c) $d = 1$ cm, $f_c = 44.8$ kHz, $\theta_a = -50°$ and $\theta_b = 0°$; (d) $d = 1.5$ cm, $f_c = 44.2$ kHz, $\theta_a = -15°$ and $\theta_b = 15°$; (e) $d = 1.5$ cm, $f_c = 45.8$ kHz, $\theta_a = -30°$ and $\theta_b = 0°$; (f) $d = 1.5$ cm, $f_c = 65.9$ kHz, $\theta_a = -10°$ and $\theta_b = 10°$.

two sound beams are transmitted at $\pm 15°$, $-30°$ and $0°$, $\pm 10°$, respectively. The additional spatial aliasing degrades the performance of the dual beam generation method. The simulation results reveal that there are boundary conditions when the two sound beams are to be transmitted using the dual beam generation method.

3. Boundary Conditions

The dual beam generation method may fail and there are approximations made in the derivation too. It is of importance to be aware of the boundary

conditions. When a steerable parametric loudspeaker is to be built up, the center frequency is determined based on the frequency response of the ultrasonic transducer. The inter-channel spacing has to be determined before the ultrasonic transducer array is assembled. Hence, the center frequency and inter-channel spacing are the design factors. On the other hand, the range of the DF and separation between the sound beams $\Delta\theta = \theta_b - \theta_a$ are performance measures that are expected to be predictable by the boundary conditions derived in this section.

The approximation made from (7) to (8) requires the condition of $c_0 >> d\left(\sin\theta_b - \sin\theta_a\right) f_d$ to be valid. To examine this condition, (8) is rewritten as

$$d\left(\sin\theta_b - \sin\theta_a\right) \approx \frac{c_0}{f_c} = \lambda_c, \tag{9}$$

where λ_c is the wavelength of the center frequency. To substitute (9) into $c_0 >> d\left(\sin\theta_b - \sin\theta_a\right) f_d$ yields

$$f_d << f_c, \tag{10}$$

which often holds in a parametric loudspeaker. However, (10) is a necessary condition. In order to find out a sufficient condition, a threshold variable is introduced as

$$\mu = \frac{d\left(\sin\theta_b - \sin\theta_a\right) f_d}{c_0}. \tag{11}$$

Using this threshold variable, the condition of $c_0 >> d\left(\sin\theta_b - \sin\theta_a\right) f_d$ is equivalent to $\mu << 1$. Moreover, (7) is simplified to

$$f_d = \frac{2\mu}{1 + \sqrt{1+\mu^2}} f_c. \tag{12}$$

The left-hand side of (12) is a quasi-linear function of μ, in particular when $\mu << 1$. If we take $\mu = 0.254$, (12) becomes $f_d = 0.25 f_c$. It determines the

upper bound of the DF that ensures the approximation from (7) to (8) to be valid. When $f_c = 40$ kHz is also given, the DF is not advised to be higher than 10 kHz. This provides the reason for the range setting of the DF in Fig. 5. It also implies that higher center frequencies are preferred for achieving wider ranges of the DF, but there is a trade-off imposed by (9).

Eq. (9) exhibits a good consistency to the spatial Nyquist sampling criterion for a uniform linear array [26]. For example, the strong requirement to avoid spatial aliasing can be derived from (9) by setting $\theta_b = 90°$ and $\theta_a = -90°$. It leads to the maximum inter-channel spacing of $d = 0.5\lambda_c$. This is also interpreted as that the spatial sampling frequency must be at least twice the cut-off frequency of the signal to be sampled. For the weak requirement to avoid spatial aliasing, the setting of $\theta_b = 0°$ and $\theta_a = -90°$ leads to the maximum inter-channel spacing of $d = \lambda_c$. In this case, the mainlobe cannot be transmitted at any angles except 0°.

The boundary condition of the dual beam generation method is derived using a similar methodology. The symmetric axis is presumed to be fixed at $\theta_s = 0°$. Therefore, when the separation between the sound beams is given, the directions of the two sound beams are simply known as $\theta_b = -\theta_a = 0.5\Delta\theta$. To avoid spatial aliasing in the observable range of angles between $\pm\theta_{observe}$, the relaxed condition is given by

$$2\sin(0.5\Delta\theta) > \frac{2\sin\theta_{observe}}{3}. \tag{13}$$

The left-hand side of (13) shows the coverage of the two sound beams in normalized angles, while the inequality means that this coverage should be at least one third of the observable range. When $\theta_{observe} = 45°$, the lower bound of $\Delta\theta$ is computed as 27.2°. This lower bound can be validated by

the simulation results. In Figs. 5(d)-(e), $\Delta\theta = 30^\circ$ is very close to but still larger than this lower bound. Therefore, there is no spatial aliasing in Fig. 5(d). But once the symmetric axis is no longer at 0°, spatial aliasing occurs in Fig. 5(e). In Fig. 5(f), since $\Delta\theta = 20^\circ$ is smaller than the lower bound, spatial aliasing is thus observed.

Furthermore, it is noted that (8) is not associated with the separation between the sound beams in angles. Instead, the center frequency is inversely proportional to the value of $\Delta\Theta = \sin\theta_b - \sin\theta_a$, which is referred to as the separation in normalized angles [19]. In pratice, $\Delta\theta$ is more likely to be given as the design factor. Figs. 5(a)-(c) show that to maintain $\Delta\theta$, the center frequency has to vary with the change of the symmetric axis θ_s. To understand the relation between $\Delta\theta$ and $\Delta\Theta$, another threshold variable is defined: υ presents the relative change of the center frequency permitted by the bandwidth or frequency response of the ultrasonic transducer.

The maximum separation in normalized angles is found as $\Delta\Theta_{max} = 2\sin(0.5\Delta\theta)$, when $\theta_b = -\theta_a = 0.5\Delta\theta$; while the minimum separation in normalized angles is found as $\Delta\Theta_{min} = 1 - \cos\Delta\theta$, when $\theta_a = -90^\circ$ or $\theta_b = 90^\circ$. However, it is of more interest to discuss a median value rather than the minimum. When $\theta_a = 0^\circ$ or $\theta_b = 0^\circ$, this median separation in normalized angles is given by $\Delta\Theta_{med} = \sin\Delta\theta$. If the center frequency has been decided based on the median separation, to achieve the maximum separation in normalized angles, the center frequency has to vary but not to exceed $1 - \upsilon$ times the decided frequency. This gives us a upper bound of the separation in angles. It is formulated by

$$\frac{\Delta\Theta_{med}}{\Delta\Theta_{max}} = \cos(0.5\Delta\theta) < 1 - \upsilon. \tag{14}$$

When $\upsilon = 10\%$, the upper bound of $\Delta\theta$ is given by 51.7°. The observations in Figs. 5(a)-(c) agree with (14) that the relative change of the center frequency is less than 9.4% when $\Delta\theta = 50°$. When $\Delta\theta = 30°$ is given in Figs. 5(d)-(e), the relative change of the center frequency is predicted by (14) to be 3.4%, which agrees well with the simulation results.

4. Experiment Results

The directivity patterns of the steerable parametric loudspeaker using the dual beam generation method were measured in an anechoic chamber with a dimension of $6\,(m) \times 3\,(m) \times 3\,(m)$. Three ultrasonic transducer arrays were assembled using different configurations as indicated in Fig. 6. All the channels were equally weighted during the measurement, but different delay amounts were implemented according to the dual beam generation method. The steerable parametric loudspeaker was mounted on a motorized rotation stage. The microphone was placed 4 m away. All directivity patterns were measured between ±45° with a resolution of 1°. The experiment results plotted in Fig. 7 were presented in normalized amplitudes.

Figs. 7(a)-(b) show the directivity patterns of the DF when the inter-channel spacing is $d = 1$ cm. The separation between the sound beams in angles is fixed at $\Delta\theta = 50°$. The two sound beams are transmitted at ±25°, −40° and 10°, respectively. In Fig. 7(b), there is about 6 dB difference between the two sound beams, due to the fact that the directivity pattern of ultrasonic transducers is not omni-directional within the observable range of angles. Figs. 7(c)-(e) show the directivity patterns of the DF when $d = 1.25$ cm and $\Delta\theta = 40°$. The two sound beams are transmitted at ±20°, −30°

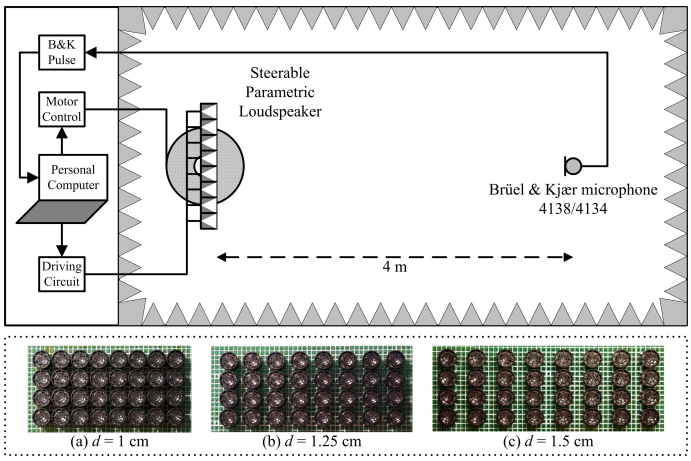

Figure 6: Measurement setup of the laboratory-made steerable parametric loudspeaker.

and 10°, −40° and 0°, respectively. To move the symmetric axis from 0° to −20°, the center frequency is increased from 40.2 kHz to 42.7 kHz. This is still predictable by (14). Figs. 7(f)-(h) show the directivity patterns of the DF when $d = 1.5$ cm and $\Delta\theta = 30°$. The two sound beams are transmitted at ±15°, −20° and 10°, −30° and 0°, respectively. The observations in Figs. 7(f)-(h) are very similar to those in Figs. 7(c)-(e). When the symmetric axis is far from 0°, partially eliminated grating lobes of the DF are observed [19] and the directivity pattern of the ultrasonic transducers causes difference in the sound pressure levels of the two sound beams. After all, the measurement results demonstrate the effectiveness of the dual beam generation method.

5. Conclusions

In this paper, the feasibility to generate two controllable sound beams using the configuration of an existing steerable parametric loudspeaker was demonstrated. Spatial aliasing of the PFs was used to generate the second

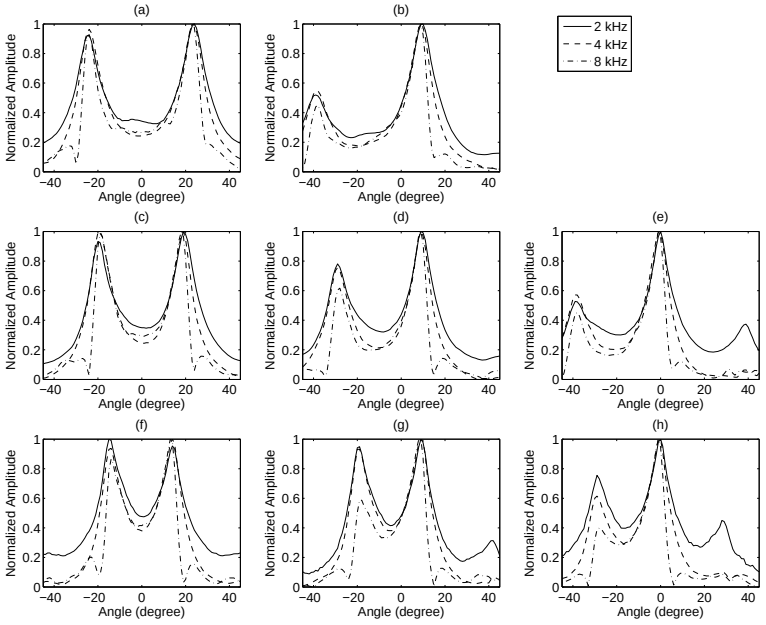

Figure 7: Measurement results: (a) $d = 1$ cm, $f_c = 40.6$ kHz, $\theta_a = -25°$ and $\theta_b = 25°$; (b) $d = 1$ cm, $f_c = 42.1$ kHz, $\theta_a = -40°$ and $\theta_b = 10°$; (c) $d = 1.25$ cm, $f_c = 40.2$ kHz, $\theta_a = -20°$ and $\theta_b = 20°$; (d) $d = 1.25$ cm, $f_c = 40.8$ kHz, $\theta_a = -30°$ and $\theta_b = 10°$; (e) $d = 1.25$ cm, $f_c = 42.7$ kHz, $\theta_a = -40°$ and $\theta_b = 0°$; (f) $d = 1.5$ cm, $f_c = 44.2$ kHz, $\theta_a = -15°$ and $\theta_b = 15°$; (g) $d = 1.5$ cm, $f_c = 44.4$ kHz, $\theta_a = -20°$ and $\theta_b = 10°$; (h) $d = 1.5$ cm, $f_c = 45.8$ kHz, $\theta_a = -30°$ and $\theta_b = 0°$.

sound beam. A concise control formula was derived and the boundary conditions were discussed in terms of the range of the DF and separation between the sound beams. Both the simulation and experiment results agreed with the boundary conditions and validated the dual beam generation method. The future work lies with the wide band implementation of the steerable parametric loudspeaker that is ready for subjective testing.

6. Acknowledgements

This work is supported by MEXT-Supported Program for the Strategic Research Foundation at Private University, 2013-2017. The detailed experiment results are also found in the first author's Ph.D. dissertation completed in Nanyang Technological University, Singapore.

7. References

[1] M. Yoneyama, J. Fujimoto, Y. Kawamo, and S. Sasabe, "The audio spotlight: An application of nonlinear interaction of sound waves to a new type of loudspeaker design," *J. Acoust. Soc. Am.* **73**, 1532–1536 (1983).

[2] P. J. Westervelt, "Parametric acoustic array," *J. Acoust. Soc. Am.* **35**, 535-537 (1963).

[3] H. O. Berktay, "Possible exploitation of non-linear acoustics in underwater transmitting applications," *J. Sound Vib.* **2**, 435-461 (1965).

[4] M. B. Bennett and D. T. Blackstock, "Parametric array in air," *J. Acoust. Soc. Am.* **57**, 562–568 (1975).

[5] C. Shi and Y. Kajikawa, "A convolution model for computing the far-field directivity of a parametric loudspeaker array," *J. Acoust. Soc. Am.* **137**, 777–784 (2015).

[6] Y. Nakashima, T. Yoshimura, N. Naka, and T. Ohya, "Prototype of mobile super directional loudspeaker," *NTT DoCoMo Tech. J.* **8**, 25–32 (2006).

[7] N. Tanaka and M. Tanaka, "Active noise control using a steerable parametric array loudspeaker," *J. Acoust. Soc. Am.* **127**, 3526–3537 (2010).

[8] K. Kimura, O. Hoshuyama, T. Tanikawa, and M. Hirose, "VITA: Visualization system for interaction with transmitted audio signals," *Proc. ACM SIGGRAPH*, Vancouver, Canada, Poster No. 54 (2011).

[9] M. Ueta, O. Hoshuyama, T. Narumi, T. Tanikawa, and M. Hirose, "JUKE Cylinder: a device to metamorphose hands to a musical instrument," *Proc. ACM SIGGRAPH*, Los Angeles, California, Poster No. 13 (2012).

[10] T. Kamakura, M. Yoneyama, and K. Ikegaya, "Developments of parametric loudspeaker for practical use," *Proc. 10th Int. Symp. Nonlinear Acoust.*, Kobe, Japan, 147–150 (1984).

[11] C. Shi, H. Mu, and W. S. Gan, "A psychoacoustical preprocessing technique for virtual bass enhancement of the parametric loudspeaker," *Proc. 38th Int. Conf. Acoust. Speech Sig. Process.*, Vancouver, Canada, 31–35 (2013).

[12] K. Aoki, T. Kamakura, and Y. Kumamoto, "Parametric loudspeaker: Characteristics of acoustic field and suitable modulation of carrier ultrasound," *Electron. Comm. Jpn* **74**, 76–82 (1991).

[13] T. Kamakura, M. Tani, Y. Kumamoto, and K. Ueda, "Harmonic generation in finite amplitude sound beams from a rectangular aperture source," *J. Acoust. Soc. Am.* **91**, 3144–3151 (1992).

[14] T. D. Kite, J. T. Post, and M. F. Hamilton, "Parametric array in air distortion reduction by preprocessing," *J. Acoust. Soc. Am.* **103**, 2871 (1998).

[15] F. J. Pompei, "The use of airborne ultrasonics for generating audible sound beams," *J. Audio Eng. Soc.* **47**, 726-731 (1999).

[16] C. Shi, E. L. Tan, and W. S. Gan, "Hybrid immersive three dimensional sound reproduction system with steerable parametric loudspeakers," *Proc. Meeting Acoust.* **19**, No. 055003 (2013).

[17] D. Olszewski, F. Prasetyo, and K. Linhard, "Steerable highly directional audio beam loudspeaker," *Proc. INTERSPEECH*, Lisbon, Portugal, 137–140 (2005).

[18] W. S. Gan, J. Yang, K. S. Tan, M. H. Er, "A digital beamsteerer for difference frequency in parametric array," *IEEE Trans. Audio Speech Lang. Process.* **14**, 1018-1025 (2011).

[19] C. Shi and W. S. Gan, "Grating lobe elimination in steerable parametric loudspeaker," *IEEE Trans. Ultrason. Ferroelectrics Freq. Control* **58**, 437-450 (2011).

[20] D. Olszewski and K. Linhard, "Highly directional multi-beam audio loudspeaker," *Proc. INTERSPEECH*, Pittsburgh, Pennsylvania, 2630–2633 (2006).

[21] S. Takeoka and Y. Yamasaki, "Acoustic projector using directivity controllable parametric loudspeaker array," *Proc. 20th Int. Cong. Acoust.*, Sydney, Australia, 921-925 (2010).

[22] K. Maeda, T. Nishino, and H. Naruse, "Horizontal and vertical sound image control using multiple parametric speakers," *J. Acoust. Soc. Am.* **131**, 3217 (2012).

[23] C. M. Darvennes and M. F. Hamilton, "Scattering of sound by sound from two Gaussian beams," *J. Acoust. Soc. Am.* **87**, 1955-1964 (1990).

[24] C. Shi and W. S. Gan, "Product directivity models for parametric loudspeakers," *J. Acoust. Soc. Am.* **131**, 1938-1945 (2012).

[25] C. Shi, "Investigation of the steerable parametric loudspeaker based on phased array techniques," Doctor of Philosophy Thesis, Nanyang Technological University, Singapore, 2013.

[26] D . H. Johnson and D. E. Dudgeon, *Array Signal Processing: Concepts and Techniques*. Prentice Hall, Upper Saddle River, New Jersey, 1993.